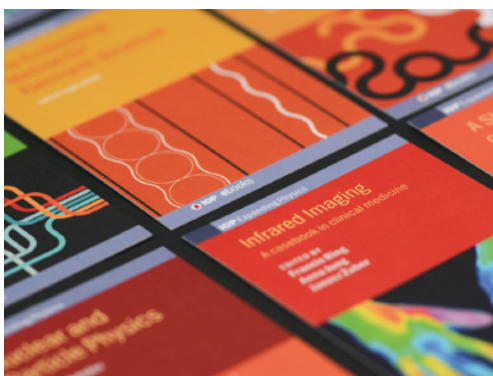


PAPER • OPEN ACCESS

## Fluorescent thermal imaging of a quench in insulated and non-insulated REBCO-wound pancake coils following a heater pulse at 77 K

To cite this article: R Gyuráki *et al* 2020 *Supercond. Sci. Technol.* **33** 035006

View the [article online](#) for updates and enhancements.



**IOP | ebooks™**

Bringing together innovative digital publishing with leading authors from the global scientific community.

Start exploring the collection—download the first chapter of every title for free.

# Fluorescent thermal imaging of a quench in insulated and non-insulated REBCO-wound pancake coils following a heater pulse at 77 K

R Gyuráki<sup>1</sup> , F Schreiner<sup>1</sup> , T Benkel<sup>1</sup> , F Sirois<sup>2</sup>  and F Grilli<sup>1</sup> 

<sup>1</sup> Karlsruhe Institute of Technology, Germany

<sup>2</sup> Polytechnique Montréal, Canada

E-mail: [roland.gyuraki@kit.edu](mailto:roland.gyuraki@kit.edu)

Received 26 September 2019, revised 19 December 2019

Accepted for publication 20 January 2020

Published 4 February 2020



CrossMark

## Abstract

High temperature superconductors (HTS)-wound coils are being developed for use in motors, generators as well as magnet applications. Determining the stability and safe operating margins of such coils still poses challenges. While the recently introduced no-insulation winding method provides a remedy for many problems, it comes with its own limitations. For comparison, we have wound two pancake coils from HTS coated conductors with the insulated and non-insulated winding techniques. Both coils were coated with a fluorescent, temperature-sensitive coating, which allowed monitoring the surface temperatures during operation. The coils were cooled to 77 K via a combination of conduction and gas cooling, and their electrical and thermal behaviour was observed in operation. Here we present the normal transition of both coils caused by an artificially introduced instability due to a surface-mounted, resistive heater element. In the insulated coil, the localized disturbance caused a local transition of the superconductor to the normal conducting state, triggering a thermal runaway. Merely the turns in contact with the artificial disturbance heated up, while the rest of the coil remained in the superconducting state. In the non-insulated coil—although a much longer heater pulse was required—the normal transition started from the weakest point of the coil (around the bobbin) and the whole coil was heating thereafter, with the centre heating more.

Keywords: thermal imaging, HTS, non-insulated coil, insulated coil, fluorescent thermal imaging

(Some figures may appear in colour only in the online journal)

## 1. Introduction

Coils wound from second generation high temperature superconductors (HTS) are a focus of research interest as they are an enabling technology for steady state magnetic field above 45 T [1]. Although HTS magnets are inherently more stable than those made out of low temperature

superconductors, the protection of HTS magnets remains a challenging topic. Defects in long length of coated conductors may cause local hot spots in HTS pancake coils that can go undetected during normal operation and develop a hot spot during transient states or due to external disturbances. The ‘self-protecting’ behaviour of non-insulated coils was reported previously in several works [2–7]; however, insulated coils are still prone to damage following local disturbances [8].

The aim of this investigation was to destabilize two test coils and observe the temporal evolution of a normal transition both thermally and electrically. To better understand the



Original content from this work may be used under the terms of the [Creative Commons Attribution 3.0 licence](https://creativecommons.org/licenses/by/3.0/). Any further distribution of this work must maintain attribution to the author(s) and the title of the work, journal citation and DOI.

**Table 1.** Properties of the non-insulated and insulated coils wound from SuperPower SCS4050 AP tape [12].

Property	Non-insulated coil	Insulated coil
Number of turns	157	157
Tape width	4 mm	4 mm
Insulation	—	50 $\mu\text{m}$ Kapton
Inner and outer diameter	30 and 85 mm	30 and 97 mm
Approximate tape length	28 m	31 m
Tape critical current <sup>a</sup>	141 A	141 A
Coil critical current <sup>b</sup>	57 and 67 A	65 and 72 A
Inductance	1.38 mH	1.49 mH
Field coefficient	3.98 mT A <sup>-1</sup>	3.6 mT A <sup>-1</sup>

<sup>a</sup> At 77 K, self-field, using the  $1 \mu\text{V cm}^{-1}$  criterion.

<sup>b</sup> At 77 K, self-field. The value was determined at an overall coil terminal voltage, calculated using the  $0.1 \mu\text{V cm}^{-1}$  and  $1 \mu\text{V cm}^{-1}$  criteria, respectively, multiplied by the total conductor length.

thermal behaviour of pancake coils and the exact development of a thermal runaway, fluorescent thermal imaging was implemented on two distinct pancake coils [9, 10]. One of the coils was wound using the conventional insulated coil winding technique while the other coil was wound without turn-to-turn insulation [11]. In this work, we show the effects of a surface-mounted heater, which we pulse for varying durations and observe the normal transition occurring inside the coil.

## 2. Measurement procedure

A non-insulated and an insulated coil were wound into pancakes with 157 turns. The coils have the same inner diameter of 30 mm. Due to the insulation, the insulated coil has a larger diameter (97 mm) than the non-insulated one (85 mm). This means that, for a given transport current, the magnetic field generated by the coils is slightly different. As a consequence, the critical current of the two coils is different as well. Their full specifications are listed in table 1.

The coils were wound onto a copper cylinder, where the last turn of the coil was deliberately left longer to be used as one of the current leads. The second current lead was a 12 mm wide HTS tape soldered with In-Ag (97%–3%) solder to the bottom of the central copper bobbin and ran under the pancake coil. For mechanical stability, the two outer turns of the coils were also soldered together. To facilitate the fluorescent thermal imaging, the surface of the coils was coated with the fluorescent solution. Simultaneously, the coil voltage was measured across the two HTS current leads and the central magnetic field was measured using an Arepoc Hall-effect sensor mounted at the centre of the coil (in the middle, on the top side of the central copper former). A finished image of the non-insulated coil is shown in figure 1. A more in-depth explanation of the experimental setup, coil winding method, cryostat and instrumentation of the non-insulated coil was presented in a previous publication [10]. The insulated coil was wound similar to the non-insulated coil, the only

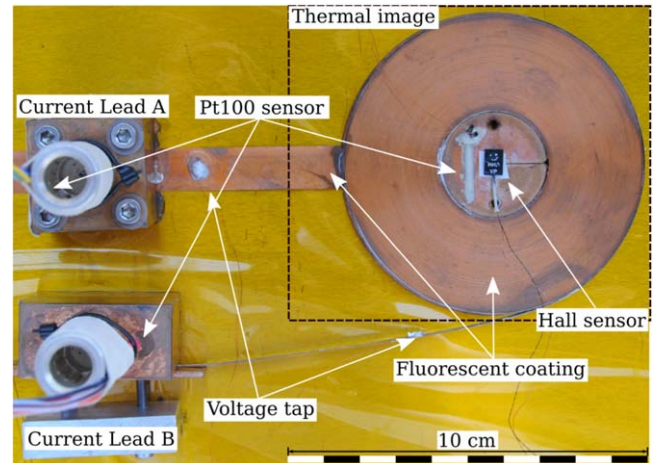


**Figure 1.** Picture of the non-insulated coil in the measurement assembly. The black rectangle indicates the thermal image as recorded by the camera. Reproduced from [10]. © IOP Publishing Ltd. All rights reserved.

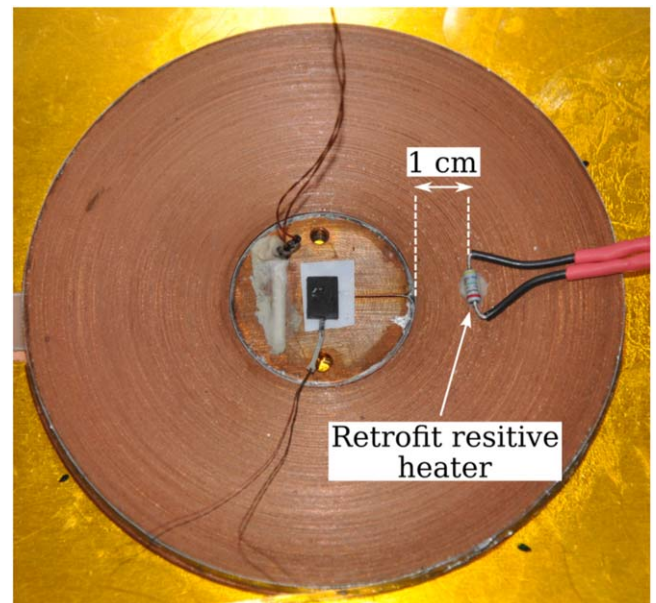


**Figure 2.** Picture of the insulated coil with a  $5 \Omega$  resistor mounted on its surface, used as a heater for creating a local disturbance.

difference being a  $50 \mu\text{m}$  thick Kapton sheet co-wound to serve as electrical insulation.

The effect of local disturbances on coil stability and quench propagation are often studied using an embedded heater inside the coil [13, 14]. Due to requirements of previous measurement, the coils presented here were instead retrofitted with a resistive heater to study similar phenomena. The heater consisted of a resistor, with a nominal resistance of  $5 \Omega$  at 77 K, mounted on the surface of the windings. The position of the heater was approximately 1 cm from the coil bobbin, on the side opposite to the 12 mm wide HTS current lead. The resistor was mounted on the surface of the coil—already coated with the fluorescent coating—using X60 two-component glue. It was in contact with only a few turns, as shown in figure 2.

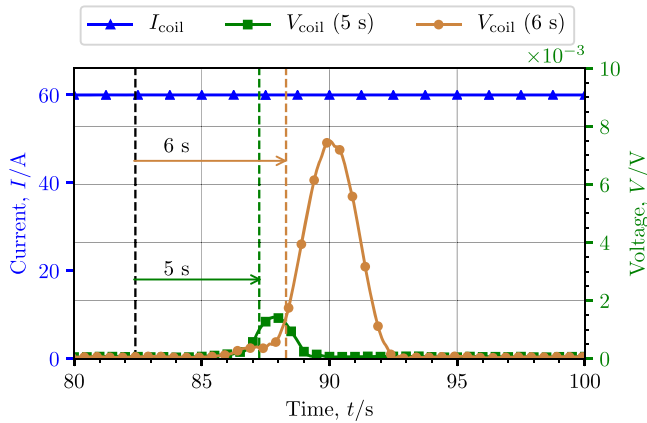


**Figure 3.** Effects of a 5 and 6 s long heat pulses at a power of 3.2 W on the insulated coil. The dashed lines indicate the heater pulse duration. The pulses were synchronized in the plot to start at 82.35 s.

The coils were cooled to 77 K in a custom-made cryostat assembly, using conduction cooling on an aluminium surface in a 77 K nitrogen gas atmosphere [10]. The camera was positioned above the coil and provided a top-down look as indicated in figure 1. Due to the absence of a liquid coolant, it is reasonable to assume that the majority of the heat dissipated in the resistor was absorbed by either the heat capacity of the resistor itself or transferred to the coil. Heat transfer to the nitrogen gas environment over the small surface of the resistor was neglected for practical purposes. Although only a small amount of glue was used for mounting the heaters, the number of turns in contact with the heater was not exactly the same in the two coils.

### 3. Insulated coil

#### 3.1. Heater pulse stability

In the experiments, the coil was ramped up to a previously validated current level, 60 A ( $\sim 83\% I_c$ ), using a Cryogenic SMS120C power supply at a ramping rate of  $5 \text{ A s}^{-1}$ . After the ramp, the coil was held steady for 60 s to rule out any unexpected transient effect (due to our uncommon cooling approach). The heater was then pulsed for a short duration (in the range of seconds) with a current of 800 mA, providing a heating power of  $\sim 3.2 \text{ W}$ . During the heater pulses, both thermal images and electrical readings were taken, and after each pulse, the coil was de-energized before the next measurement.

For heater pulse durations of up to 2 s, the coil voltage remained stable and the thermal imaging showed barely detectable fluctuations caused by the heater itself, not related to the coil operation. This indicates that the superconductor itself did not incur losses due to a transfer into the dissipative state (in any significant manner). For increased heater pulse durations, the coil voltage rose and also recovered on its own after the disturbance was stopped. The results of electrical measurements of 5–6 s long heater pulses are shown in figure 3. The two heater pulses caused an approximately

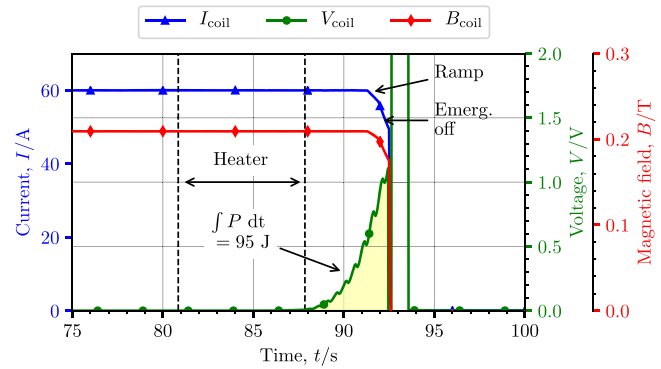


**Figure 4.** Electrical measurement of the quench in the insulated coil caused by a 7 s long heat pulse at a heater power of 3.2 W. A manual ramp down is indicated in the figure followed by an ‘emergency off’ of the power supply to protect the coil.

2 and 8 mV signal across the coil terminals, after which the coil promptly recovered. During these two measurements, still no localized heating was detected in the coil.

#### 3.2. Thermal runaway

At a pulse length of 7 s, the coil was no longer able to recover from the heat input and a normal transition was recorded. This is shown in figure 4. A detectable voltage rise was measured during the heater pulse. However, the voltage continued to rise even after the heater pulse ended. Simultaneously, in the thermal images, it is visible that the windings touched by the heater started to transit into the normal conducting regime and incurred Joule losses, followed by heating, as shown in figure 5. The heater pulse started approximately at 81 s, as shown in figure 5, where the heater is causing optical artefacts, which are actually not relevant to the thermal imaging. In figure 5, 2 s after the heater pulse ended, distinct heating is visible in the coil around the heater at a coil voltage of  $\sim 0.2 \text{ V}$ . The temperature in the windings then peaked at 92 s (figure 5), where only the turns directly in contact with the heater were affected. At 97 s figure 5 shows the cooling down of the involved turns. As expected, the electrical and thermal insulation provided by the Kapton layer between the turns greatly reduces the heat propagation in the radial direction of the insulated coil. As a consequence, merely the windings in direct contact with the surface-mounted heater were heating. It is also visible that heating was present mostly around the heater, diminishing progressively along the length of the turn with an overall hot zone of approximately 70% of the circumference of the involved windings. These results show—from a thermal perspective—the existing problem of protecting insulated HTS coils as developed hot spots do not propagate considerably inside the body of the coil, but are restricted to a small fraction of the windings.

Upon seeing the high voltages developed in the coil at approximately 92 s, a manual ramp down was initiated in the experiment to protect the coil. However, the voltage rise did not stop immediately and the power supply’s ‘emergency off’ engaged at around 93 s and dropped the current to zero. The

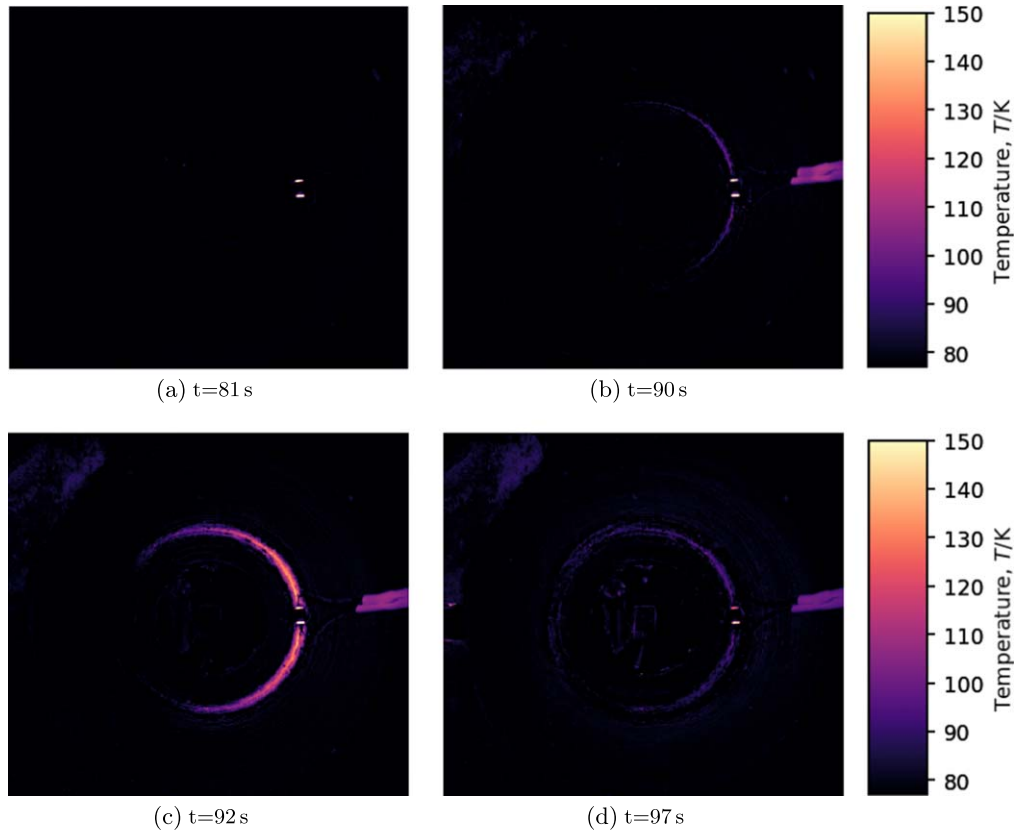


**Figure 5.** Thermal images of the normal transition in the insulated coil caused by a 7 s long heater pulse. Note that discolouring of the heater and cables is noise and not related to the thermal imaging.

energy released inside the coil due to the superconducting-to-normal transition was calculated by integrating the electrical power dissipation in the coil, starting from the heater firing until the emergency discharge (over the period 80.85–92.6 s)

$$\int_{t_0}^{t_1} P dt = \int_{80.85s}^{92.6s} I \cdot V dt = 95 \text{ J.} \quad (1)$$

The coil was further tested in subsequent measurements by both operating it closer to its critical current and letting the normal transition develop further, up to voltages of 5 V (this constitutes the limit of the current supply at which the ‘emergency off’ is automatically triggered). The normal transition was found to be qualitatively similar in all such scenarios, with the normal transition starting from the position of the heater disturbance and propagating solely in the turns directly in contact with the heater.

After several heat pulses at 7 s with a steady operating current close to the coil’s critical current and triggered discharges, the coil’s critical current was found to be unchanged, indicating no permanent damage.

#### 4. Non-insulated coil

##### 4.1. Heater pulse stability

The non-insulated coil was also tested using heater pulses, using a heater almost identical to that of the insulated coil. Due

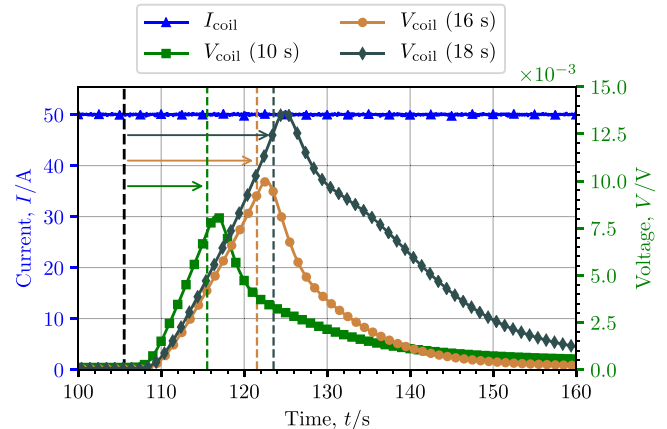


**Figure 6.** Voltage response of the NI coil to heater pulses of 3.2 W for durations of 10, 16 and 18 s. The pulses were synchronized in the plot to start at 105.5 s.

to experimental considerations, in the measurements shown here, the coil was ramped to a slightly lower current, i.e. ~75% of  $I_c$  (50 A). The ramping rate was kept at  $5 \text{ A s}^{-1}$  and upon reaching the target current level, the coil was then given 90 s to stabilize. The heater was then pulsed with the same current of 800 mA for various durations. Figure 6 shows a summary of the effects of heater pulses applied to the NI coil for durations of 10, 16 and 18 s. Coil terminal voltages were measured in the range of 8 mV, where longer pulses caused a progressively larger electrical voltage across the coil’s terminals. After each

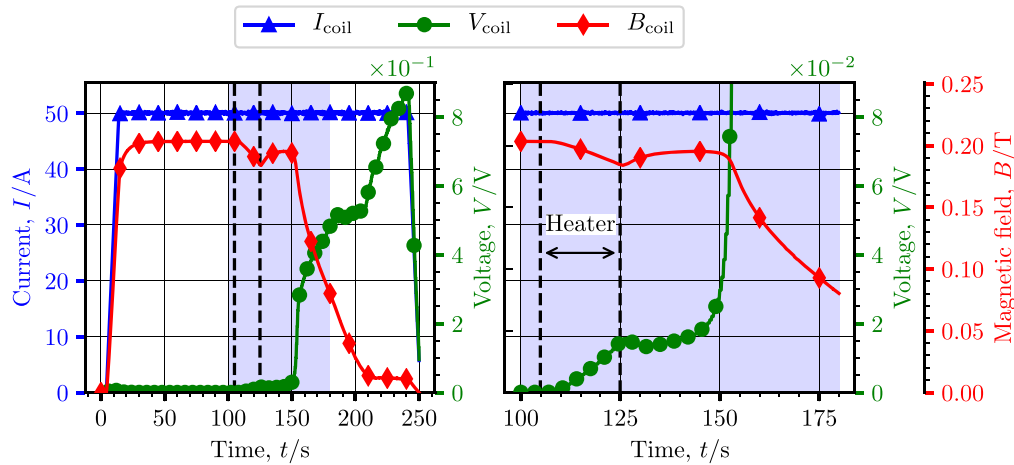


**Figure 7.** Electrical measurement of the quench in the non-insulated coil caused by a 20 s long heater pulse at a power of 3.2 W. The highlighted area is shown in greater resolution. Note the changed scale of the measured voltage.

heater pulse, the coil recovered to steady state operation. The rate of voltage rise was higher for the experiment with the 10 s heater pulse than in the other two measurements.

The time to full recovery took significantly longer than in the case of the insulated coil, however, the heater pulse was also 2–3 times longer.

It is also important to point out that while in the case of the insulated coil the magnetic field remained unchanged during the disturbances, in the non-insulated coil, the magnetic field did decrease during the heater pulses. This was expected, since the current redistribution due to the disturbance caused more current to bypass parts of the coil.

#### 4.2. Thermal runaway

When increasing the heater pulse duration to 20 s, a runaway was observed as shown in figure 7.

During the heater pulse, a distinct voltage rise was visible across the coil terminals. However, after stopping the heater disturbance the coil showed signs of self-recovery initially. This effect is visible on the recovering coil voltage in figure 7 after 125 s as well as on the increasing magnetic field. The combination of these two signals indicate currents transferring back into the spiral path of the coil. However, a few seconds later ( $\sim 130$  s) the coil voltage started to rise again and the magnetic field did not increase any further towards the previous plateau. Yet another  $\sim 5$  s later a sharp voltage rise was recorded, indicating that part of the coil was transitioning from superconducting to normal conducting state. After this rapid voltage rise and drastic reduction in the magnetic field, further rise in voltage became more linear and the magnetic field fell and stabilized at  $\sim 10\%$  of its original value. Following the initial sharp voltage rise, indicating a normal transition inside the windings, the coil was operated for another 100 s before de-energizing. The peak heating power reached before ramping down was around 40 W, as estimated from  $P = I \cdot V$ . After the experiment, the critical current was re-measured and found to be unchanged, indicating that no permanent damage was done to the coil.

Thermal images recorded during the normal transition of the coil are shown in figure 8. In this measurement, even though the heater was positioned 1 cm away from the coil's centre (figure 2), no considerable heating was visible during the heater pulse (figure 8). Then in figure 8, it is visible that the thermal runaway has in fact started from around the coil's centre (the bobbin) and propagated outwards, starting from the moment of rapid coil voltage appearance. Thereafter, in figure 8, the temperature around the centre increased and started propagating further into the body of the coil. Finally, at 241 s in figure 8, just before ramping down the coil, most of the coil was above 100 K, with the centre being close to 130 K. In this figure it is also visible that the 12 mm wide HTS current lead was also heating, and reaching above 150 K. The cooling of this current lead was sub-optimal and hence such an effect was expected.

The results indicate that while the normal transition in the non-insulated coil was initially triggered by a long heat load at a localized disturbance, the transition itself did not originate from this position. Instead, the current redistribution inside the coil caused the weakest part of the coil to begin a transition, which then spread across the coil. In this coil design, the weakest point was the centre of the coil around the copper bobbin, where the magnetic field is the strongest and hence degrades the critical current of the conductor to the highest extent [15]. Simultaneously, Joule losses were present due to a soldered joint between the copper bobbin and the HTS coil itself, thereby further reducing the critical current density. After the initial normal transition of superconducting windings around the centre of the coil, the coil voltage rise became more linear, with more current flowing through the turn-to-turn contact resistances. This effect is also clear in the thermal recording, where the centre of the coil heats up rapidly, followed by a more gradual heating in the body of the coil.

This experiment revealed a remarkable resemblance to a thermal runaway when the coil was operated in an overcurrent regime, as presented previously [10]. We believe this is due to the fact that no larger heating power than  $\sim 3.2$  W could be applied in the current measurement approach. This potentially

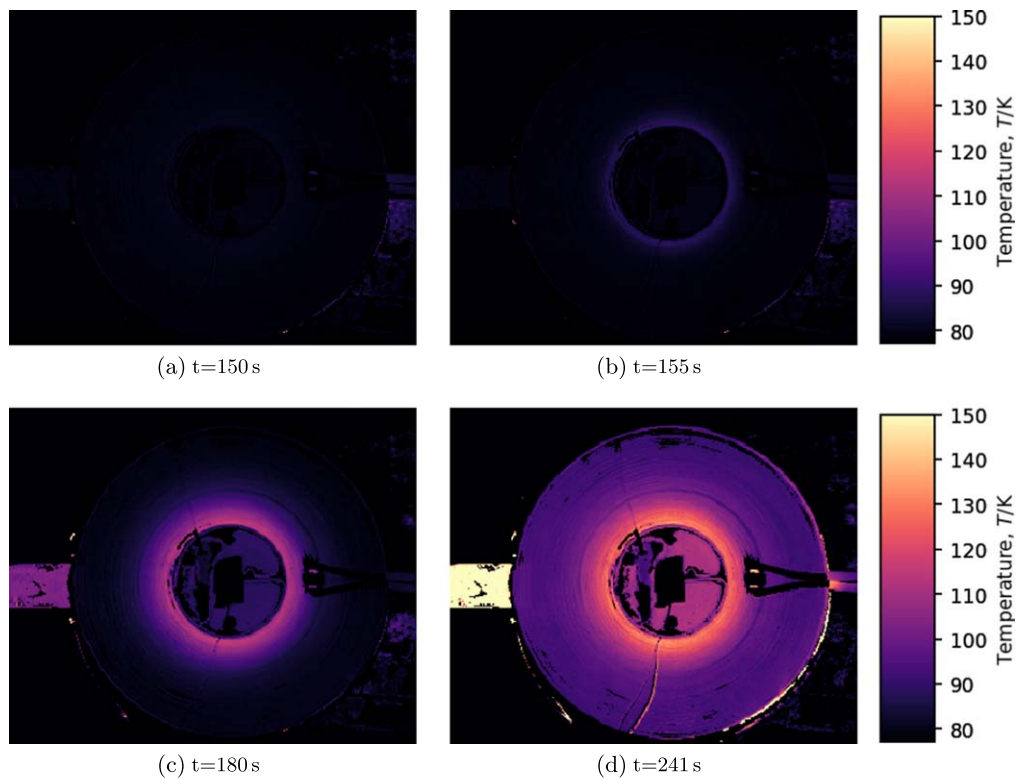


**Figure 8.** Thermal images of the normal transition in the the non-insulated coil during 20 s heater pulse measurement. Note that discolouring of the heater and cables is noise and not related to the thermal imaging.

led to a slower current redistribution, resulting in a normal transition around the weakest part of the coil (after turning off the heater).

## 5. Conclusion

The stability and normal transition of an insulated and a non-insulated pancake coil with an identical number of turns was investigated using both electrical measurements and thermal imaging, in the context of a local disturbance caused by a surface-mounted heater element. A superconductor-to-normal transition was observed in the insulated coil following a heat pulse duration of 7 s at 3.2 W. The thermal imaging revealed strongly localized heating in the coil, caused by Joule losses around normal transitioning section of the superconductor. The heating was further constrained by the electrical and thermal insulation between the turns resulting from the use of an insulating Kapton film. The temperature of the superconductor directly around the location of the disturbance approached 150 K, before the coil was de-energized.

In the non-insulated coil, a normal transition was first observed when applying a 20 s long heat pulse. While a rising coil voltage was visible during the heat pulse, afterwards the coil showed initial signs of recovery. Keeping the coil still under load, a normal transition began a few seconds later. The normal transition started from the centre of the coil, around the bobbin, where the magnetic field was the strongest and a resistive joint was also present. The coil was operated for 100 s after the appearance of an initial normal transition of the

superconductor. During this time, the entire coil heated above 100 K with the innermost turns being closer to 130 K.

The experiments show that a localized disturbance in an insulated coil indeed causes strong localized heating due to the local transition of the superconductor and strongly reduced thermal conduction in the radial direction. Compared to this, in a non-insulated coil, a localized disturbance does not necessarily cause a local hot spot. The available resistive heater limited the maximum applicable heating power. Therefore, it is currently unsure if a higher heating power, applied for a shorter duration, would cause a qualitatively different normal transition in a non-insulated coil. This, however, requires changes in both our experimental assembly and procedure, and hence remains a topic of future research.




## Acknowledgments

The authors would like to acknowledge the support from the Superwind and FASTGRID projects (European Commission Grant No. 721019). This work was supported in part by the DFG (German Research Foundation) under Grant NO 935/1-1, and in part by the National Natural Science Foundation of China under Grant 51761135120.

## ORCID iDs

R Gyuráki  <https://orcid.org/0000-0001-9648-5556>

F Schreiner  <https://orcid.org/0000-0003-0146-2322>

T Benkel  <https://orcid.org/0000-0002-7589-2686>  
 F Sirois  <https://orcid.org/0000-0003-0372-9449>  
 F Grilli  <https://orcid.org/0000-0003-0108-7235>

## References

- [1] Hahn S *et al* 2019 45.5-tesla direct-current magnetic field generated with a high-temperature superconducting magnet *Nature* **570** 496–9
- [2] Choi Y H, Hahn S, Song J B, Yang D G and Lee H G 2011 Partial insulation of GdBCO single pancake coils for protection-free HTS power applications *Supercond. Sci. Technol.* **24** 125013
- [3] Hahn S, Park D K, Voccio J, Bascunan J and Iwasa Y 2012 No-Insulation (NI) HTS Inserts for >1 GHz LTS/HTS NMR Magnets *IEEE Trans. Appl. Supercond.* **22** 43024
- [4] Hahn S, Kim Y, Song J, Voccio J, Ling J, Bascunan J and Iwasa Y 2014 A 78-mm/7-T multi-width no-insulation ReBCO magnet: key concept and magnet design *IEEE Trans. Appl. Supercond.* **24** 1–5
- [5] Yanagisawa Y, Sato K, Yanagisawa K, Nakagome H, Jin X, Takahashi M and Maeda H 2014 Basic mechanism of self-healing from thermal runaway for uninsulated REBCO pancake coils *Physica C* **499** 40–4
- [6] Song J B, Hahn S, Licrevisse T, Voccio J, Bascuñ J and Iwasa Y 2015 Over-current quench test and self-protecting behavior of a 7 T/78 mm multi-width no-insulation REBCO magnet at 4.2 K *Supercond. Sci. Technol.* **28** 114001
- [7] Kim S *et al* 2017 Quench behavior of a no-insulation coil wound with stainless steel cladding REBCO *Supercond. Sci. Technol.* **30** 075001
- [8] Awaji S, Watanabe K, Oguro H, Miyazaki H, Hanai S, Tosaka T and Ioka S 2017 First performance test of a 25 T cryogen-free superconducting magnet *Supercond. Sci. Technol.* **30** 065001
- [9] Gyuráki R, Sirois F and Grilli F 2018 High-speed fluorescent thermal imaging of quench propagation in high temperature superconductor tapes *Supercond. Sci. Technol.* **31** 34003
- [10] Gyuráki R, Benkel T, Schreiner F, Sirois F and Grilli F 2019 Fluorescent thermal imaging of a non-insulated pancake coil wound from high temperature superconductor tape *Supercond. Sci. Technol.* **32** 105006
- [11] Hahn S, Park D K, Bascuñán J and Iwasa Y 2011 HTS pancake coils without turn-to-turn insulation *IEEE Trans. Appl. Supercond.* **21** 1592–5
- [12] SuperPower 2014 SuperPower 2G HTS Wire Specifications *Technical Report* SuperPower Inc. ([http://www.superpower-inc.com/system/files/SP\\_2G+Wire+Spec+Sheet\\_2014\\_web\\_v1\\_0.pdf](http://www.superpower-inc.com/system/files/SP_2G+Wire+Spec+Sheet_2014_web_v1_0.pdf))
- [13] Song H, Gagnon K and Schwartz J 2010 Quench behavior of conduction-cooled YBa<sub>2</sub>Cu<sub>3</sub>O<sub>7-δ</sub> coated conductor pancake coils stabilized with brass or copper *Supercond. Sci. Technol.* **23** 065021
- [14] Kim S B, Saitou A, Joo J H and Kadota T 2011 The normal-zone propagation properties of the non-insulated HTS coil in cryocooled operation *Physica C* **471** 1428–31
- [15] Zhang X, Zhong Z, Ruiz H S, Geng J and Coombs T A 2016 General approach for the determination of the magneto-angular dependence of the critical current of YBCO coated conductors *Supercond. Sci. Technol.* **30** 025010